GA–A23815

QUIESCENT H–MODE PLASMAS IN THE DIII–D TOKAMAK

by

K.H. BURRELL, M.E. AUSTIN, D.P. BRENNAN, J.C. DeBOO, E.J. DOYLE, P. GOHIL, C.M. GREENFIELD, R.J. GROEBNER, L.L. LAO, T.C. LUCE, M.A. MAKOWSKI, G.R. McKEE, R.A. MOYER, T.H. OSBORNE, M. PORKOLAB, T.L. RHODES, J.C. ROST, M.J. SCHAFFER, B.W. STALLARD, E.J. STRAIT, M.R. WADE, G. WANG, J.G. WATKINS, W.P. WEST, and L. ZENG

NOVEMBER 2001

DISCLAIMER

GA–A23815

QUIESCENT H–MODE PLASMAS IN THE DIII–D TOKAMAK

by

K.H. BURRELL, M.E. AUSTIN,* D.P. BRENNAN, J.C. DeBOO, E.J. DOYLE,† P. GOHIL, C.M. GREENFIELD, R.J. GROEBNER, L.L. LAO, T.C. LUCE, M.A. MAKOWSKI,‡ G.R. McKEE,§ R.A. MOYER,¶ T.H. OSBORNE, M. PORKOLAB,△ T.L. RHODES,† J.C. ROST,△ M.J. SCHAFFER, B.W. STALLARD,‡ E.J. STRAIT, M.R. WADE,# G. WANG,† J.G. WATKINS,◊ W.P. WEST, and L. ZENG†

This is a preprint of a paper to be presented at the 8th IAEA Technical Committee Meeting on H–Mode Physics and Transport Barriers, Toki, Japan, September 5–7, 2001, and to be published in the *Plasma Physics and Controlled Fusion.*

*University of Texas, Austin, Texas.
†University of California, Los Angeles, California.
‡Lawrence Livermore National Laboratory, Livermore, California.
§University of Wisconsin, Madison, Wisconsin.
¶University of California, San Diego, California.
△Massachusetts Institute of Technology, Cambridge, Massachusetts.
#Oak Ridge National Laboratory, Oak Ridge, Tennessee.
◊Sandia National Laboratory, Albuquerque, New Mexico.

Work supported by
the U.S. Department of Energy under Contract Nos. DE-AC03-99ER54463, W-7405-ENG-48, DE-AC05-00OR22725, DE-AC04-94AL85000 and Grant Nos. DE-FG03-97ER54415, DE-FG03-01ER54615, DE-FG03-96ER54373, DE-FG03-95ER54294, DE-FG02-90ER54084 and DE-FG02-94ER54235 APTE

GENERAL ATOMICS PROJECT 30033
NOVEMBER 2001

ABSTRACT

H–mode operation is the choice for next step tokamak devices based either on conventional or advanced tokamak physics. This choice, however, comes at a significant cost for both the conventional and advanced tokamaks because of the effects of edge localized modes (ELMs). ELMs can produce significant erosion in the divertor and can affect the beta limit and reduced core transport regions needed for advanced tokamak operation. Recent experimental results from DIII–D have demonstrated a new operating regime, the quiescent H–mode regime, which solves these problems. We have achieved quiescent H–mode operation which is ELM-free and yet has good density control. In addition, we have demonstrated that an internal transport barrier can be produced and maintained inside the H–mode edge barrier for long periods of time (>3.5 seconds or >25 energy confinement times τ_E). By forming the core barrier and then stepping up the input power, we have achieved $\beta_N H_{89} = 7$ for up to 10 times the τ_E of 160 ms. The $\beta_N H_{89}$ values of 7 substantially exceed the value of 4 routinely achieved in standard ELMing H–mode. The key factors in creating the quiescent H–mode operation are neutral beam injection in the direction opposite to the plasma current (counter injection) plus cryopumping to reduce the density. Density control in the quiescent H–mode is possible because of the presence of an edge MHD oscillation, the edge harmonic oscillation, which enhances the edge particle transport while leaving the energy transport unaffected.

1. INTRODUCTION

Because of its superior energy confinement, H–mode operation is the choice for next step tokamak devices based either on conventional [1] or advanced tokamak [2,3] physics. This choice, however, comes at a significant cost for both the conventional and advanced tokamaks because of the effects of edge localized modes (ELMs). The standard view is that ELMing H–mode operation is required for density and impurity control. However, the ELMs produce pulsed divertor heat and particle loads which can lead to rapid erosion of the divertor plates [4]. In addition, for the advanced tokamak, giant ELMs couple to core MHD modes (e.g neoclassical tearing modes) and thus reduce the beta limit. Furthermore, giant ELMs can destroy the reduced transport core which is needed for the profile optimization required for advanced tokamak operation [5]. Recent experimental results from DIII–D have demonstrated a new operating regime which solves these problems. We have achieved quiescent H–mode operation which is ELM-free and yet has good density and radiated power control. In addition, we have demonstrated that an internal transport barrier can be produced and maintained indefinitely inside the H–mode edge barrier, producing an operating regime dubbed the quiescent double barrier (QDB) regime. The QDB plasmas have significantly improved plasma performance relative to that of standard ELMing H–mode.

The key factors in creating the quiescent H–mode operation are neutral beam injection in the direction opposite to the plasma current (counter injection) plus cryopumping to reduce the density. These have allowed long pulse, ELM-free operation with constant density and radiated power levels for periods up to 3.5 seconds or about 25 global energy confinement times τ_E. There is no known plasma physics limitation which would prevent this quiescent operation from being extended to steady state. The duration in present experiments was limited by the choice of plasma current flat top and neutral beam pulse length. The duration of the reduced core transport exceeds that of the quiescent H–mode edge, since the core transport reduction begins before the ELMs go away and the quiescent H–mode is established. Normalized performance in terms of β_N and H_{89} improves with increasing neutral beam input power. Here $\beta_N = \beta / \left(I / aB_T \right)$ is the normalized beta [2,3] and H_{89} is the confinement enhancement factor relative to the ITER89P scaling [1]. By forming the core barrier and then stepping up the power, we have achieved $\beta_N H_{89} = 7$ for up to 10 times the τ_E of 160 ms. The $\beta_N H_{89}$ values of seven substantially exceed the value of four routinely achieved in standard ELMing H–mode.

Density and radiated power control in the quiescent H-mode is possible because of the presence of an edge MHD oscillation, the edge harmonic oscillation, which enhances the edge particle transport while leaving the energy transport unaffected. The qualitative behavior induced by this mode is similar to that reported for the quasi-coherent mode in enhanced D_α (EDA) operation in the C-Mod tokamak [6-8]; however, the details of the two modes are quite different [9].

The present paper focuses on the physics of the quiescent H–mode edge. Other publications at this conference [10] and elsewhere [9,11] discuss the core physics of the QDB regime.

2. QUIESCENT H–MODE EDGE

2.1. Basic Nature of Quiescent H–mode

Figure 1 illustrates the basic behavior of quiescent H–mode shots run during the 2000 and 2001 campaigns on DIII–D. After an initial ELMing phase, the bursts on the divertor D_α signal disappear, leading to a quiescent phase, which is the source of the name for this operating regime. Unlike the monotonic increase seen in standard ELM-free H–mode, the line-averaged density [Fig. 1(b)], pedestal electron density [Fig. 1(i)] and radiated power [Fig. 1(g)] are essentially constant during the quiescent phase. This indicates that the particle transport at the plasma edge is rapid enough to provide density control. As is seen in Fig. 1(f), the nature of the oscillations detected by the magnetic pickup loops changes when the ELMs cease, from a bursting behavior to a much more continuous oscillation. This is the edge harmonic oscillation (EHO) which will be discussed extensively later in the paper. Our data indicate that the presence of this oscillation is what usually provides the enhanced edge particle transport. Although the EHO gives enhanced particle transport, it has little effect on the energy transport. The edge temperature and pressure gradients in the quiescent H–mode are as large as those in the ELMing H–mode. The global energy confinement time in these quiescent phases is at or above the standard H–mode level.

Figure 1 also illustrates that the quiescent H-mode can operate for long periods of time. This particular shot is ELM-free for about 3.5 seconds or about 25 τ_E. The quiescent phase terminates only because the plasma current and neutral beam power were preprogrammed to ramp down at 5 seconds into the shot.

Although most of the shots in the 2000 and 2001 campaigns have an ELMing phase prior to the quiescent phase, this sequence does not always occur. During the 1999 campaign, we ran shots which were limited on the centerpost of the vacuum vessel for the first 1800 ms of the discharge. The plasma was then changed to a diverted, pumping shape. In these cases, the quiescent phase sometimes arose directly out of the standard ELM-free phase just after the L to H transition.

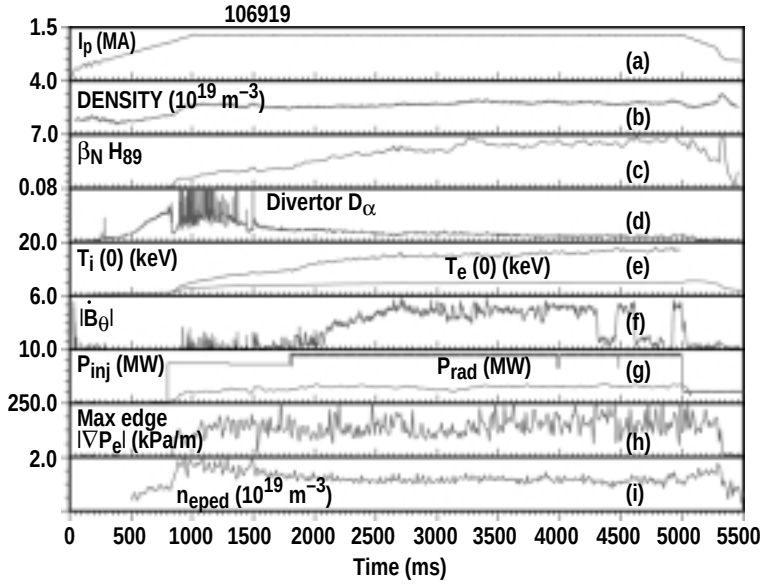

Fig. 1. Time history of a quiescent H–mode shot. (a) plasma current, (b) line-averaged density, (c) product of normalized beta and energy confinement time enhancement factor H_{89}, (d) divertor D_α emission, (e) central ion and electron temperature, (f) $|\dot{B}_\theta|$ from magnetic probe, (g) total injected neutral beam power and total radiated power, (h) maximum edge electron pressure gradient and (i) the pedestal electron density. The latter two are determined from a hyperbolic tangent fit to the electron pressure and density measured by Thomson scattering. Toroidal field is 2.0 T. The scale on each box of the graph ranges from zero to the maximum value given on the figure.

2.2. Conditions For Quiescent H–mode

Quiescent H–mode plasmas were discovered in DIII–D in 1999 when we combined counter-injection with cyropumping to lower the plasma density [12,13]. In experiments conducted so far, we need neutral beam powers above about 3.0 MW to access this operating regime. Line-averaged densities are typically in the range of 2 to $3\times10^{19}\,\mathrm{m}^{-3}$ while the local density at the top of the H–mode edge pedestal is around 1 to $2\times10^{19}\,\mathrm{m}^{-3}$. For comparison, line averaged and pedestal densities are both around $6\times10^{19}\,\mathrm{m}^{-3}$ in unpumped ELMing H–mode at 1.3 MA plasma current. The exact density boundary has not been established as a function of the other plasma parameters. However, data clearly show that increased gas puffing or pellet injection into previously established quiescent plasmas leads to the destruction of the edge harmonic oscillation and a return of ELMs. The quiescent phase can be re-established once the edge density perturbation decays. Quiescent H–modes are typically operated with no extra particle fueling beyond that provided by the neutral beam injection. Modifying the cryopumping efficiency by changing the plasma shape can be used to increase the density to a certain extent while still remaining in quiescent H–mode. The highest pedestal electron density seen to date in quiescent H–mode is $4\times10^{19}\,\mathrm{m}^{-3}$. In cases like that shown in Fig. 1, the

total exhaust rate is about 1×10^{21} deuterons/s; 40% of these go to the pump, the rest go to the walls.

As is shown in Fig. 2, the quiescent H–mode operates at a lower pedestal electron density and a higher pedestal electron temperature than most of the H–modes in DIII–D. The pedestal ion temperature and pressure are typically well above those in ELMing H–mode [9,11,13].

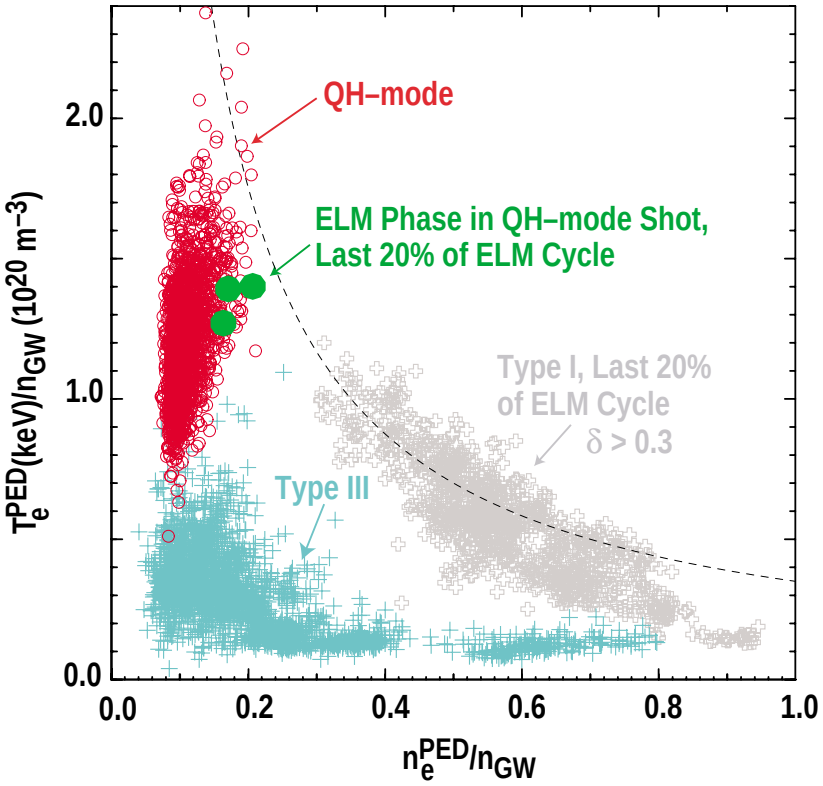

Fig. 2. Plot of pedestal electron temperature versus pedestal electron density with both axes normalized to the Greenwald density, $n_{GW} = I_p/\pi\, a^2$. In this formula, n_{GW} is in units of 10^{20} m^{-3}, I_p is the plasma current in MA and a is the plasma minor radius in meters. The dashed line on the figure shows the shape of trajectories of constant pedestal electron pressure in this space. Most of the Type I and Type III ELM data on this plot come from a range of co-injected plasma conditions. A few points (solid symbols) show the edge conditions where Type I ELMs occur in the counter injected shots which later exhibit quiescent H–mode. These come, for example, from times between 1000 and 1400 ms in shots like that in Fig. 1. For constant n_{GW} (i.e. constant current and minor radius) the dashed line in the figure is a line of constant pressure.

A third necessary condition for robust quiescent H–mode operation is a sufficiently large distance (>10 cm) between the plasma edge and the vacuum vessel wall on the low toroidal field side of the discharge. This is probably related to use of counter neutral beam injection. For counter injection, there are a significant number of neutral beam produced

fast ions which exist outside the plasma edge on the low field side. It appears that interaction of these particles with the vessel wall is detrimental to long-term quiescent operation. Transient quiescent operation with outer gaps as small as 5 cm is possible for a few hundred milliseconds. Exactly why this interaction is detrimental is not known. One possibility is that extra gas evolved from the wall owing to this interaction affects the quiescent phase the same way that an extra gas puff does.

Single-null divertor configurations were used in all of the long duration quiescent H–mode experiments to date. We have a few examples of transient double-null quiescent H–modes lasting a few hundred milliseconds but we have not yet attempted long duration double-null operation. The direction of the ion ∇B drift relative to the divertor X–point does not matter; quiescent operation has been seen in both cases. We have seen quiescent H–modes over entire range of triangularity ($0.16 \le \delta \le 0.75$) and safety factor q ($3.7 \le q \le 5.8$) explored to date. Most of our work has been done with plasma current I_p in the range $1.0 \le I_p\,(\mathrm{MA}) \le 1.6$ and toroidal field B_T in the range $1.8 \le B_T\,(\mathrm{T}) \le 2.1$ with neutral beam powers up to 13.5 MW. We also have quiescent H-mode examples at 0.67 MA and 0.95 T.

2.3. Steep Edge Gradients

Since the divertor D_α trace in Fig. 1(d) superficially looks like a return to L–mode after the ELMs cease, it is important to establish that the quiescent phase truly is an H–mode. The edge density and temperature gradients in the quiescent phase are as steep as the ones in the ELMing phase of the discharge [9,11,13]. Since it is the edge transport barrier which is the *sine qua non* of the H–mode, the quiescent phase is indeed H–mode. The continuation of the steep edge gradients into the quiescent H–mode is also illustrated in Fig. 1(h) where we see that the maximum edge electron pressure gradient does not change when the ELMs cease and the quiescent phase begins.

2.4. Particle Flux Enhanced by Edge Harmonic Oscillation

A key feature of the quiescent H–mode is the constant density and radiated power levels in the absence of ELMs. This quite an astonishing result, give the worldwide observation of continuous density and impurity accumulation in standard ELM-free H–modes and VH–modes [14]. This accumulation in standard ELM-free H–mode and VH–modes is due to the very low particle flux out of these plasmas. Since the quiescent H–mode does not exhibit this accumulation, the outward particle flux must be substantially larger. A fundamental question, then, is how this comes about.

Measurements of divertor D_α radiation and line average density show that divertor recycling increases and plasma density decreases after the onset of the edge harmonic oscillation [9]. As is illustrated in Fig. 3, the ion saturation current to Langmuir probes in the divertor plates [15] in contact with the scrape-off layer plasma exhibit the same harmonic frequency structure as the magnetic probe data [9]. This demonstrates directly that the edge harmonic oscillation drives particle flux into the divertor. Probes in the private flux region on the other side of the separatrix do not show the edge harmonic oscillation. The EHO has also been seen on currents flowing from the scrape-off layer plasma through the divertor plates.

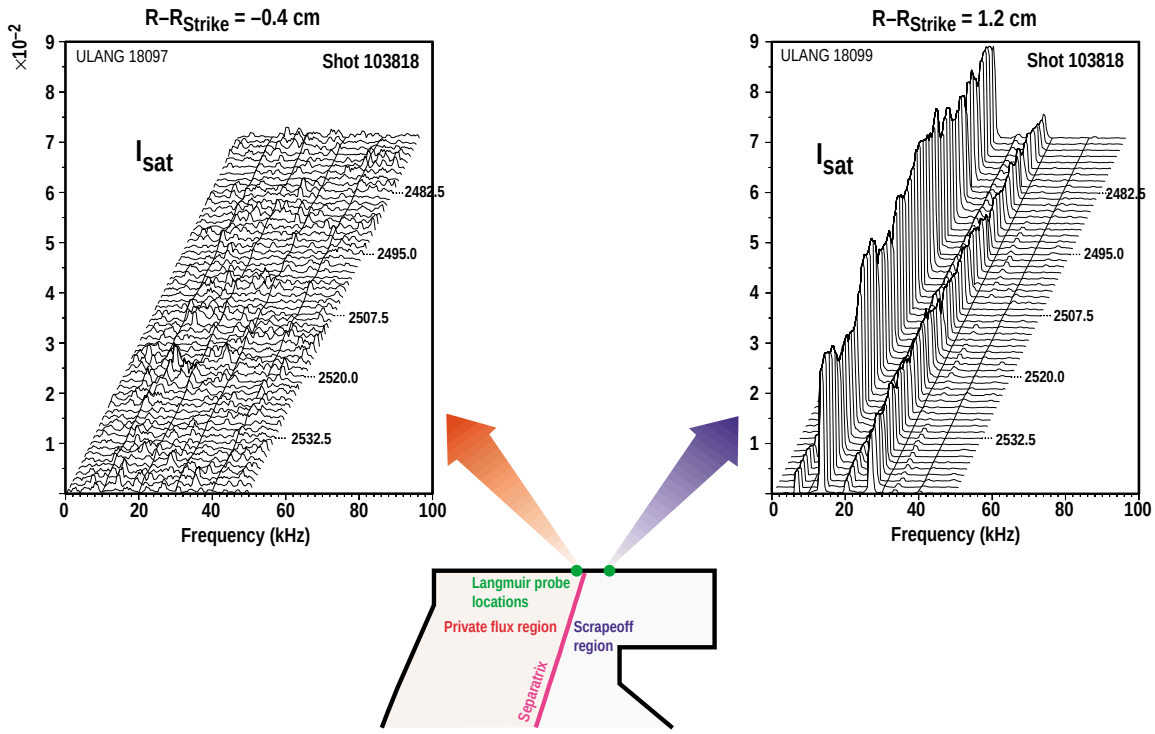

Fig. 3. Plots of ion saturation current from Langmuir probes in the divertor plates. Data are Fourier analyzed to produce plots as a function of frequency for a whole time sequence. As indicated by the sketch, one probe is in contact with the scrape-off layer plasma while the other is in contact with the private flux plasma. Note that the vertical scales differ by a factor of 100 for the two plots. The edge harmonic oscillation dominates the signal from the probe in contact with the scrape off layer plasma; it is undetectable on the private flux probe. Plasma conditions are 1.3 MA, 2.0 T.

Although the vast majority of the shots with density control have the edge harmonic oscillation, we have a single shot (106956) without it that still exhibits controlled density. In this shot, there is a core tearing mode instead. Observations in other, co-injected discharges with cryopumping show that the plasma density decreases after the onset of the core tearing mode. This demonstrates that these modes can also push particles across the separatrix and, ultimately, into the cryopump. As is discussed in more detail in the

next section, other signatures of the tearing mode and the edge harmonic oscillation are quite different, demonstrating that these are distinct types of modes. Their main similarity is their effect on particle flux.

2.5. Nature of the Edge Harmonic Oscillation

Although it was first seen on the magnetic probes, the edge harmonic oscillation also has density and temperature fluctuations associated with it. Density fluctuations have been seen using beam emission spectroscopy (BES) [16], reflectometry [17,18], FIR scattering [19] and phase contrast imaging (PCI) [20] while the temperature fluctuations have been seen on the electron cyclotron emission (ECE) diagnostic [21]. The density and magnetic oscillations both show multiple harmonics in the range of 1 to 10 [9]. Because the oscillation is weaker 2–3 cm inside the separatrix where the electron cyclotron emission is black-body, we have only seen the fundamental and the first one or two harmonics on the temperature oscillation. Analysis with the DIII–D magnetic probe array shows that each distinct frequency has its associated toroidal mode number n. In other words, the fundamental frequency f has an n=1 toroidal mode number, 2f has an n=2 toroidal mode number, etc. If one looks at the actual oscillation on the magnetic probes, for example, it is clear that the oscillation is periodic but not sinusoidal. The multiple harmonics/multiple n numbers are simply the Fourier harmonics needed to describe such a non-sinusoidal oscillation. The density, temperature and magnetic oscillations are highly coherent with each other. However, the precise ratio of the amplitude of the various harmonics differs between the various signals. The change in phase with toroidal angle detected by the magnetic probes shows that the edge oscillation propagates in the same direction as the neutral beams.

As has been shown previously [9], the mix of Fourier harmonics involved in the edge harmonic oscillation is variable. The mix can vary from shot to shot or even within one shot. Surprisingly, the measured edge pressure gradients do not change significantly even when the mix of toroidal harmonics changes as long as the oscillation is present. This can be seen in Fig. 1(f) and 1(h). The changes in magnetic probe amplitude in Fig. 1(f) after 4000 ms are due to the edge harmonic oscillation switching from n=2 dominated to n=3 dominated and back several times. As is shown in Fig. 1(h), the edge pressure gradient does not change when this happens.

When the edge harmonic oscillation ceases, the plasma returns to standard ELM-free conditions and the edge density rises. ELMs follow within roughly 100 ms or less. Such a cessation sometimes occurs, for example, when we deliberately decrease the gap between the plasma and the wall in order to scan the plasma edge across the various edge

diagnostics. If the EHO ceases, there is typically a delay of 50 to 100 ms between the time of minimum gap and the cessation.

The edge harmonic oscillation is quite obvious in counter injected discharges. Since its discovery [12,13], we have also noticed that a similar oscillation sometimes exists in co-injected H–mode discharges. This oscillation is only seen infrequently with co-injection but it has the same multi-harmonic character as with counter injection. The initial observation of the co-injected EHO were in unpumped, low power discharges [9]. During the 2001 campaign, we found a number of cases with cryopumping where the EHO existed in co-injected discharges with input powers up to 14 MW. All cases where we have seen the edge harmonic oscillation in co-injected discharges have large ELMs. There is as yet no sign of quiescent H–mode with co-injection. In counter injected shots, when the edge harmonic oscillation first turns on after an ELM, the frequency drops. However, for co-injected discharges, the frequency rises when the oscillation first turns on either after an ELM or in the initial ELM-free phase after the L to H transition. For both co- and counter-injected cases, the edge harmonic oscillation rotates toroidally in the same direction as the neutral beams.

2.6. Edge Harmonic Oscillation and Tearing Modes

As mentioned previously, both the EHO and tearing modes can affect particle confinement. This similarity lead to a hypothesis that the EHO was a tearing mode localized at the $q=3$ or $q=4$ surface in the plasma. Additional support for this hypothesis was the analysis of the toroidal and approximate poloidal mode number associated with the magnetic portion of the EHO [9], which suggested that the mode might be located at these surfaces. To investigate this, we have analyzed the data from the BES radial array to determine the variation of the phase and coherence between the various BES channels. For the data taken in 2001, the BES views were arranged in one long radial array (22 chords, 1.1 cm apart) on the vessel midplane and two short arrays (5 chords each) 5.5 or 11 cm below the midplane.

A typical example of such analysis is seen in Fig. 4. This is for an n=2 dominated edge harmonic oscillation in the same shot as is shown in Fig. 1. The radial phase plot shows that the oscillation occurs earliest near or outside the separatrix. The phase variation with radius is consistent with radial propagation both inwards and outwards from this location. The phase convention used has larger phases for earlier phenomena. More important for the test of the tearing mode idea is the smooth variation of phase with radius.

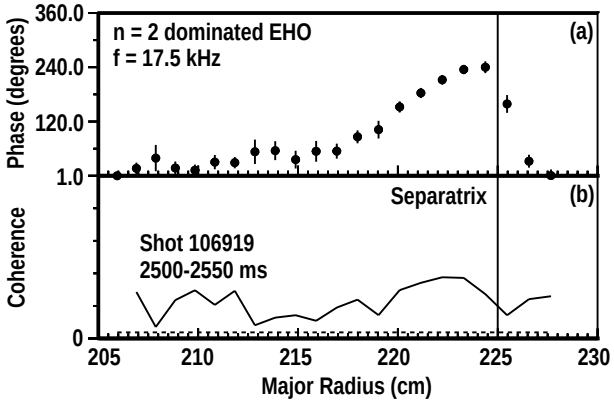

Fig. 4. Plot of radial dependence of (a) phase and (b) coherence for density fluctuations detected by the 22 channel beam emission spectroscopy array. The reference channel for all these is the leftmost point on the plots. The convention for the phase has oscillations with higher phase values occurring earlier.

Most of the quiescent H–mode shots do not exhibit core tearing modes because counter neutral beam current drive usually holds the minimum safety factor $q_{\min}$ to values above 1.3. However, we have one shot which shows both the EHO and a core tearing mode. A transient locked mode lowered $q_{\min}$ just enough for the core mode to be triggered. The BES signals for this shot are shown in Fig. 5. The classic signature of the core tearing mode is shown in Figs. 5(a) and (b). There is a 180 degree phase reversal across a layer where the coherence becomes very low. MHD equilibrium analysis shows that this point is quite close to the $q=5/2$ surface; toroidal mode number of 2 and poloidal mode number of 5 are consistent with analysis of the magnetic probe data. A very important feature of the phase plot for the tearing mode is the constant phase with radius outside of the tearing layer. The EHO portion of Fig. 5 as well as Fig. 4 show that the EHO phase varies continuously with radius inside the separatrix, quite unlike that of the tearing mode.

If we made the hypothesis that the EHO was a tearing mode localized to the $q=3$ or $q=4$ surface, we would expect the phase plot show a 180 degree phase change at that point and to be constant from that point on out into the scrape-off layer. For shots like those in Figs. 4 and 5, the $q=3$ surface is about 6 cm inside the separatrix and the $q=4$ surface is 2 to 3 cm inside the separatrix. No such constant phase signature is seen in the EHO data in Figs. 4 and 5. Accordingly, it appears that the EHO is not the same MHD phenomenon as a core tearing mode.

The difference in the phase variation of the EHO with radius in Figs. 4 and 5 deserves comment. In Fig. 4, the phase continues to drop as one goes into the plasma from the separatrix while in Fig. 5 it first drops and then rises again. This is probably an artifact of the effect of the edge localized density oscillation on the neutral beam itself. The edge density oscillation can impose a modulation on the neutral beam itself by changing the

beam attenuation. This affects the BES measurement little in the region where the density oscillation is large because the common mode due to beam modulation is small compared to the local effect of the density oscillation. However, deeper into the plasma, this common mode effect can compete with the density oscillation located there. Depending on which one of these dominates, one can get phase plots deeper into the plasma which either increase or decrease with distance.

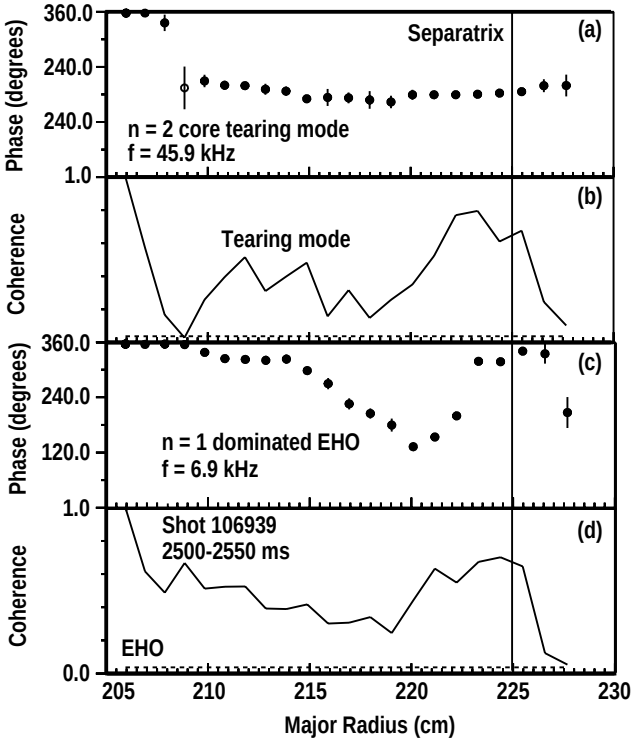

Fig. 5. Plot of the radial dependence of phase and coherence of density oscillations detected by the beam emission spectroscopy system for a shot exhibiting, at different frequencies, both an n=2 core tearing mode [(a) and (b)] and an n=1 dominated edge harmonic oscillation [(c) and (d)]. The radial structure of the phase is quite different for the two. For each plot, the reference point for phase or coherence is the leftmost point.

2.7. ELM Stabilization

A key question for the quiescent H–mode is: Why do the ELMs go away? At present, we do not have the final answer to this. We have examined several hypotheses and have found reasons to question all of them. Testing others will require improvements in diagnostics or theory.

An early hypothesis was that the edge harmonic oscillation was so virulent that it lowered the edge pressure gradient below the value needed to create ELMs. However, the plots in Fig. 1(h) and previously published results [9] show that the edge pressure

gradient in the quiescent phase is at least as large as that in the ELMing phase. Accordingly, this hypothesis is not consistent with the data. If one thinks in terms of comparing the edge pressure gradient to some critical gradient [19], one must conclude that the stability boundary had moved because of some change in the edge plasma conditions.

Another hypothesis was that the edge harmonic oscillation represents the MHD precursor to an ELM which has been saturated by an unspecified mechanism at a level below that needed to cause the transient ergodization which gives the confinement degradation and consequent D_α burst associated with the fully developed ELM. There are certainly cases where the edge harmonic oscillation persists until an ELM occurs; this can happen, for example, after the edge harmonic oscillation has started but before the ELMs are completely suppressed. However, there are also a number of cases where the edge harmonic oscillation stops and an ELM does not take place for several tens of milliseconds. These cases were discussed in Section 2.5. This behavior seems inconsistent with the concept of a precursor. It is a strange precursor which goes away well prior to the onset of the phenomenon which it is supposed to trigger.

Additional evidence against the idea that the edge harmonic oscillation is a saturated ELM precursor comes from the co-injection observations. As is common with co-injected plasmas, for these cases the ELM precursors are observed to rotate in the electron drift direction (opposite to the beam direction). The edge harmonic oscillation in both co- and counter-injection cases rotates in the direction of the neutral beams. This observation strongly suggests that the edge harmonic oscillation and the ELM precursors are different modes.

Because the question of ELM stabilization is so important, it is worth speculating on possible causes. One possibility is finite Larmor radius stabilization caused by the different ion orbits associated with counter-injection and/or the much higher edge ion temperature. A second possibility is stabilization owing to changes in the edge current density; theory indicates that edge current density is a key parameter in overall MHD stability of the edge [22]. A third possibility is stabilization by large rotational [23] or electric field shear. As is shown in Fig. 6, one of the unique features of the quiescent H–mode is the very different electric field structure near the plasma edge in the quiescent phase compared to the ELMing phase of the same shot or to the ELM-free phase of a co-injected shot. Indeed, the H–mode electric field well in the quiescent H–mode discharges is the deepest yet seen. Unfortunately, full assessment of the role of electric field shear in ELM stabilization requires a major extension of MHD stability theory.

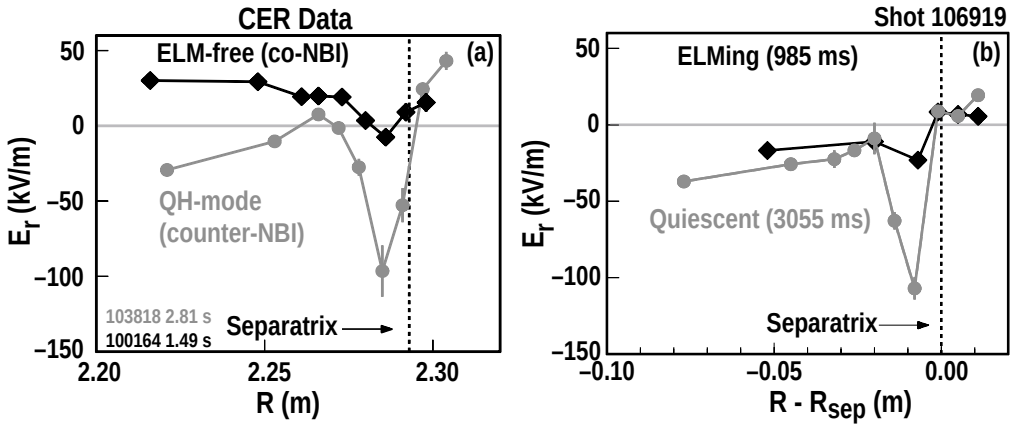

Fig. 6. Structure of the edge radial electric field near the separatrix in H–mode discharges. The electric field is determined by charge exchange spectroscopy. (a) Comparison of the edge radial electric field in a counter-injected quiescent H–mode discharge (103818) and the ELM-free phase of a co-injected discharge (100164) at roughly similar plasma currents (1.3 vs. 1.6 MA), input powers (7.1 vs. 7.3 MW) and toroidal fields (2.0 vs. 1.8 T). (b) Comparison of the edge radial electric field during the ELMing (◆) and quiescent phases (●) of the same shot as in Fig. 1.

3. CONCLUSIONS

By utilizing counter neutral beam injection plus density reduction through cryopumping, we have produced quiescent H–mode plasmas in DIII–D. These discharges have an ELM-free H–mode edge with no D_α bursts and no pulsed heat load to the divertor. Owing to the presence of the edge harmonic oscillation, edge particle transport in this regime is sufficiently rapid that discharges can be operated with constant density and constant radiated power levels in spite of the absence of ELMs. In addition, a reduced transport core plasma fits quite naturally with the quiescent H–mode edge owing to the lack of ELMs and absence of sawteeth. Although we have considerable information about the edge harmonic oscillation, a theory to explain this mode does not yet exist. Finally, a theory to explain why the ELMs disappear in these discharges also remains to be created.

4. REFERENCES

[1] ITER Physics Basis Document, *Nucl. Fusion* **39** 2137 (1999).
[2] Taylor T S et al. 1994 *Plasma Physics and Controlled Fusion Research* **36** B229
[3] Taylor T S 1996 *Plasma Physics and Controlled Fusion* **39** B47
[4] Leonard AW 1999 *J. Nucl. Mater*. **266-269** 100
[5] Burrell K H 2001 2001 *Rev. Sci. Instrum.* **72** 906.
[6] Greenwald M et al 1999 *Phys Plasma* **6** 1943
[7] Greenwald M et al 2000 *Plasma Physics and Controlled Fusion* **42**, A263
[8] Hubbard A et al 2001 *Phys Plasma* **8** 2033
[9] Burrell K H et al 2001 *Phys Plasma* **8** 2153
[10] Greenfield C M et al 2001 "The Quiescent Double Barrier Regime in DIII–D," submitted to Plasma Physics and Controlled Fusion
[11] Doyle E J et al 2001 " The Quiescent Double Barrier Regime in the DIII–D Tokamak" submitted to Plasma Physics and Controlled Fusion
[12] Burrell K H et al 1999 *Bull. Am. Phys. Soc.* **44** 127
[13] Groebner R J et al 2001 *Nucl. Fusion* **41** (to be published)
[14] Jackson G L et al 1992 *Phys. Fluids* **B 4** 2181
[15] Buchenauer D et al 1990 *Rev. Sci. Instrum.* **61** 2873
[16] McKee G R et al 1999 *Rev. Sci. Instrum.* **70** 913
[17] Rhodes T L et al 1998 *Plasma Physics and Controlled Fusion* **40** 1575
[18] Doyle E J et al 2000 *Plasma Physics and Controlled Fusion* **42** A237
[19] Rettig C L et al 1990 *Rev. Sci. Instrum.* **61** 3010
[20] Coda S et al 1992 *Rev. Sci. Instrum.* **63** 4974
[21] Wang Z et al 1995 Proc. 9th Workshop on Electron Cyclotron Emission and Electron Cyclotron Heating, Borrego Springs, California p. 427
[22] Ferron J R et al 2000 *Phys. Plasma* **7** 1976
[23] Miller R L et al 1995 *Phys. Plasma* **2** 3676

5. ACKNOWLEDGMENTS

\Work supported by U.S. Department of Energy under Contract Nos. DE-AC03-99ER54463, W-7405-ENG-48, DE-AC05-00OR22725, DE-AC04-AL85000, and Grants DE-FG03-97ER54415, DE-FG03-01ER54615, DE-FG03-96ER54373, DE-FG03-95ER54294, DE-FG02-90ER54084, and DE-FG02-94ER54235APTE.